

# Bisphenol A Removal from Aqueous Solution Using Waste Agarwood Activated Carbon: Kinetic and Isotherm Investigation of Adsorption Process

Mosa Jafer, Husni Ibrahim\*, Y.H. Taufiq-Yap

Received: 16 July 2019 ▪ Revised: 17 August 2019 ▪ Accepted: 18 September 2019

**Abstract:** Presently, it is difficult to prepare inexpensive water pollutant adsorbents of promising efficiency based on natural source-derived activated carbons (AC). This work investigated the properties of agarwood-synthesised AC (agar AC) of high potential. Displaying an expansive surface area, this carbon was examined in terms of its kinetics and isotherms associated with adsorption of bisphenol A. The preparation of agar AC involved a three-stage process of chemical activation, comprising carbonisation, treatment with sulphuric acid and activation, with agarwood branch serving as precursors. The highest BET surface area of the synthesised agar AC was 1092 m<sup>2</sup>/g, while the highest absorptivity of the activated carbon under conditions of 50°C, three hours, pH 7 and 1 wt. % carbon dosage was 430 mg/L. Exhibiting an endothermic and spontaneous character, adsorption was observed to comply with the pseudo-second-order with Langmuir and Freundlich adsorption isotherms. In the context of water purification, bisphenol A adsorption could be adequately and inexpensively achieved with this agar AC, which can also be used again following a renewal with great effectiveness of extraction.

**Keywords:** Activated carbon, Bisphenol A, Adsorption, Kinetics, Langmuir/Freundlich, Water Quality.

## INTRODUCTION

Water as essential resources for human and survival of all ecosystem. These resources are under threat due to the introduction of Xenoestrogens (endocrine disrupting compounds) into the environment *via* anthropogenic activities. This compound makes water unsafe for human consumption and dangerous to aquatic organisms. The BPA is one of the endocrine disturbing compounds, widely used as raw materials in the producing of PVC polymer, polycarbonate plastic, epoxy resins and food containers, with annual production beyond 3.8\*10<sup>6</sup> ton (Michałowicz, 2014). This plasticizer was found in the engineered and natural environment (Wu 2019). BPA is classified as a substance of very high concern that poses severe injury to the environment and public health according to the environmental protection agency (EPA, US) (Lassouane et al., 2019). BPA is confirmed to be linked with various health problems like reproductive disorder, breast cancer, obesity, neurological and cardiovascular diseases (Chen et al., 2018; Shafei et al., 2018). Hence, the need to constantly monitor this organic content in water and removed the BPA in wastewater.

Biodegradation (Dai et al., 2016), osmotic and microfiltration (Zhu & Li, 2013), adsorption (Choi & Kan, 2019), advanced oxidation (Pachamuthu et al., 2017) are reported techniques of BPA removal from water. Amongst listed purification techniques, adsorption by activated carbons stands out as the most

---

Mosa Jafer, Department of Biology, Faculty of Science and Mathematics, Universiti Pendidikan Sultan Idris, Tanjung Malim, Malaysia.

Ministry of Education, Iraq, Baghdad, Iraq.

Husni Ibrahim\*, Department of Biology, Faculty of Science and Mathematics, Universiti Pendidikan Sultan Idris, Tanjung Malim, Malaysia. Email: husni@fsm.ups.edu.my

Y.H. Taufiq-Yap, Catalysis Science and Technology Research Centre, Faculty of Science, Universiti Putra Malaysia, UPM Serdang, Selangor, Malaysia.

efficient method due to its design simplicity and easy exploitation. Nanomaterials including graphene, fullerenes and carbon nanotubes have been applied as effective adsorbent materials for the uptake of BPA. However, these nanomaterials are without shortcomings such as expensive production cost and generation of toxic sludge. Hence, the urge to search for cheap and environmentally friendly carbon source as an alternative. Choi and Kan (2019) studied the removal of BPA by adsorption onto alfalfa-based biochar. The adsorption isotherm fitted well with the Freundlich model and Langmuir adsorption capacity was 62.7 mg/g (Choi & Kan, 2019). Genc et al. used surfactant-modified natural zeolite to remove the bisphenol-A from aqueous solution onto. The maximum BPA uptake was 86.21 mg/g at pH 7 (Genç et al., 2017). Though, the sorption capacity of these agro wastes and natural adsorbents were found comparable to other bio-adsorbent but lower than adsorption capacity of commercial carbon.

The purpose of this study was to identify an efficient precursor for agarAC production to achieve the adsorption of bisphenol inexpensively and effectively. Thus, AC synthesis via chemical activation was undertaken with agarwood waste branch. Furthermore, consideration was given to the extent to which the adsorption potential was affected by the parameters of original pH, adsorption time and temperature. The outcomes of the experiment constituted a basis for the examination of how the agar AC was impacted by the adsorption optimization, thermodynamics and kinetics of the bisphenol-A removal. The findings of the present study can make a valuable contribution to the achievement of an inexpensive agar AC of high efficiency to eliminate the issue of bisphenolA contamination and gain a detailed comprehension of adsorption isotherms and kinetics.

## **MATERIALS AND METHODS**

### **Preparation of Activated Carbons**

Agarwood was first cleaned from the dust and the other impurities by washing with hot water, followed by scrapping and rinsed with tap water for several times. The washed Agarwood were dried in an oven at 100 °C for 48 hours to remove adhering water. Dry Agarwood was ground into a fine powder by a milling machine. The powder was sieved through a metal sieve(200 mesh) and then calcined under N<sub>2</sub> flow of 10 cc/min up to 700 °C ~1h at a rate of 10°C min<sup>-1</sup>; then, the calcination was increased to 750 °C under a CO<sub>2</sub> flow at the rate of 5 °C min<sup>-1</sup> for 4 hours. The carbon was treated with H<sub>2</sub>SO<sub>4</sub> at 180 °C for 24 hours, followed by purification using copious amounts of deionized water until the pH of the solution became neutral. The powder was subsequently dried at 100 °C for 12 hours. Then, the carbon was calcined at 450 °C at the rate of 5 °C min<sup>-1</sup> for 3 hours under nitrogen gas. All chemicals and reagent used are of analytical grade.

### **Characterization of Activated Carbon**

The BET surface area analyser (V\_sorb 4800P) was used to investigate the surface area and porosity of the agar AC based on N<sub>2</sub> adsorption and under relative pressure of between 0.00 and 1.00. Prior to BET analysis, the samples were subjected to degassing at 150°C for one day under vacuum. The functional groups on the agar AC surface were identified by employing an FTIR Spectroscopy (Perkin Elmer Spectrum 65 FT IR Spectrometer), with finely ground KBr comprising approximately 0.5 wt.% of the activated carbon samples being used for infrared spectra transmission.

The KBr and the samples had been previously left to dry at 100°C for one day. In all cases, the spectrograms represented the average of thirty scans, with wavelengths varying between 300 and 4000 cm<sup>-1</sup>. XRD (Shimadzu XRD-6000) was used to scientifically analyse the crystal configuration and the physical qualities of the agar AC sample minerals. For this purpose, XRD was applied across the 2θ range 5° to 80° and 2° per minute of scanning rate. Molecules can be effectively determined via Raman spectroscopy. In the present case, this involved employing a laser micro Raman system (Horiba JobinVyon, LabRam HR) with the diffusion of 488-nm monochromatic light to detect the graphitic character of the synthesised carbon from the G, D and 2D band shift. The FESEM (HITACHI, Japan) was employed to analyse the agar AC in terms of its surface morphology and structure. The sample was burned in a muffle furnace at a temperature of 575°C for a period of five hours in order to find out the overall quantity of ash that AC contained.

### **Adsorption Studies**

Analytical grade bisphenol A solution in concentrations of 10, 25, 50, 100, 250 and 500 mg/L were used to conduct bisphenol A adsorption studies on the synthesised agar AC. An HPLC helped to approximate the bisphenolA concentration in the first and last solutions. Batch mode experiments conducted in a glass tube with a volume of 50 ml enabled assessment of the efficiency of the synthesised

agar AC for adsorbing bisphenol A. Attention was also paid to how the ability of agar AC to adsorb bisphenol A was affected by contact time and original pH at an ambient temperature of 30°C. Agar AC samples weighing 1 wt.% were employed under conditions of 30°C and 4.12 pH to assess how the adsorption capability was affected by the original pH. The procedure involved the addition of ACs in 50 ml bisphenol A with 250 mg/l concentration at the original pH of 3, 7 and 9. A pH meter (Sartorius) table-top were used for the measurement of the pH of the samples, which was kept unchanged by enhancing the original solution with solutions of 0.01 (N) HCl and 5% of NH<sub>4</sub>OH. To determine how the adsorption capability was impacted by the temperature at a particular pH (pH=7) (the highest adsorption capacity is attained at that pH) for an equilibrium time of 24 hours.

### Kinetics and the Adsorption Equilibrium Studies

Batch experiments were conducted at ambient temperature, with 1 wt.% of activated carbon being added to a specific volume of bisphenol A solutions with different concentrations (10 to 500 mg/L) in a 100 ml falcon tube. A shaker was used to agitate the mixtures until equilibrium was attained. A range of time frames was used to conduct the tests. The adsorption efficiency of agar AC was determined by using HPLC to determine the left concentration of bisphenol-A in the solutions following adsorption. Commercial AC was evaluated in an identical manner. To determine the percentage of BPA assimilation equation (1) was applied:

$$\%R = \frac{C_o - C_e}{C_o} \times 100 \quad (1)$$

And to determine the BPA adsorption amount equation 2 was applied:

$$q_e = V \frac{C_o - C_e}{W} \quad (2)$$

In the above, the original liquid-phase concentration of bisphenol-A, measured in mg/L, is denoted by  $C_o$ , while the equilibrium BPA liquid-phase concentration is denoted by  $C_e$ ; the quantity of adsorbed BPA, measured in mg/g is denoted by  $q_e$ , while the solution volume, measured in L, and the weight of the employed agar A Cadsorbent, measured in g, are respectively denoted by  $V$  and  $W$ .

## RESULTS AND DISCUSSION

### Materials Characterization

N<sub>2</sub> adsorption/desorption isotherms were employed to analyse the specific surface area and porosity of the carbon produced from agarwood through pyrolysis and secondary activation, as well as of the commercial carbon (Figure 1a). Associated with type IV isotherms based on the definition by the International Union of Pure and Applied Chemistry (IUPAC), the occurrence of hysteresis loop was exhibited by the isotherm both prior to and after agar carbon was activated (El-aassar et al., 2016). Pre-activation, agar carbon had a BET surface area of 669.72 m<sup>2</sup>/g, while post-activation, its BET surface area was 1092 m<sup>2</sup>/g. Amorphous carbon with cylindrical pore channels that are clearly outlined is classified by IUPAC as H1 histogram and is illustrated in Figure 2a. Furthermore, less amorphous carbon with homogeneously sized rigid bulk particles (Chine et al., 2011) and weak interplays with N<sub>2</sub> represents the H3 histogram shown in Figure 2b.

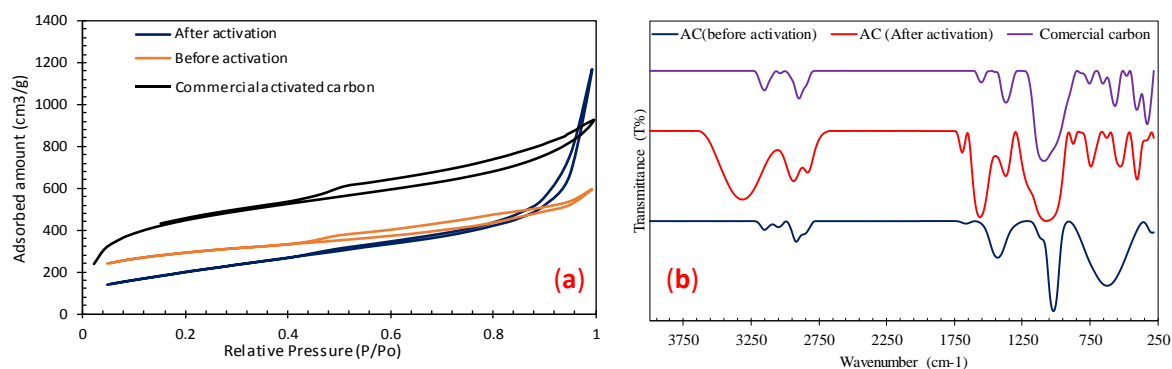


Figure 1: a) N<sub>2</sub> adsorption/desorption isotherms of carbon and b) Fourier-transform infrared spectroscopy (FT-IR) analysis

Figure 1b illustrates the FTIR analysis of the AC functional groups. Hydroxyl group, carboxylic group, alkenes, alkynes and aldehydes were among the functional groups that were identified. BPA adsorption from the liquid phase is based on the presence of such functional groups in agar AC. C-H stretching of alkane at  $2898\text{-}2912\text{ cm}^{-1}$  and aldehyde  $2826\text{-}2847\text{ cm}^{-1}$  was displayed by every sample. Meanwhile, robust O-H alcohol stretching or N-H stretching of  $\text{R-NH}_2$  might explain the peaks that all ACs displayed at  $3200\text{-}3550\text{ cm}^{-1}$ . Furthermore, the peak at  $1655\text{-}1691\text{ cm}^{-1}$  which is referred to C=O stretching of aldehyde. The robust O-H carboxylic acid group stretching might have been the reason for the marked broad peak exhibited by the samples at  $3300\text{ cm}^{-1}$  post-activation. Robust peak of nitro compounds and aromatic amines (N-O) stretching was suggested by the peaks displayed in the agar AC post-activation and by commercial carbon at  $1360\text{-}1368\text{ cm}^{-1}$ . N-C=S represented a marked peak at  $1590\text{ cm}^{-1}$  displayed by the agar AC post-activation, while C-S and C=S respectively represented the marked peak at  $743\text{ cm}^{-1}$  and marked peak at  $743\text{ cm}^{-1}$  displayed by agar AC following the second activation.

Figure 2 illustrates the FESEM imaging of carbon. The action of sulphuric acid during pyrolysis led to the formation of a heterogeneous surface (honeycomb-like structure) displaying porosity (micropore and mesopore) in the agar pyrolyzed carbon with no ulterior activation. Besides pore formation, pyrolysis at  $700^\circ\text{C}$  caused the elimination of a considerable proportion of volatiles as well as the degeneration of cellulose, hemicelluloses and lignin compound from the precursor. Moreover, the mesopore volume was enhanced at the expense of the micropore volume as the pore was attacked by the acid when ulterior activation with pure 98% sulphuric acid was performed (Figure 3a). As shown in Figure 3, agar AC had well-defined pores on its surface. The agar AC surface exhibited visible pores with clear pore walls (Alalwan et al., 2018; Idan et al., 2017). One reason for this may be the discharge of the elements displaying volatility and the breakdown of sulphuric acid groups in agar AC as an outcome of the integrated processes of pyrolysis, carbonisation and sulfonation. Furthermore, the latter could be explained in terms of the powerful acid attack associated with sulfonation and causing additional volatile substances to be released in agar AC. The relatively expansive BET surface area displayed by agar AC might be the outcome of this. Conversely, micropores were exhibited by the commercial AC.

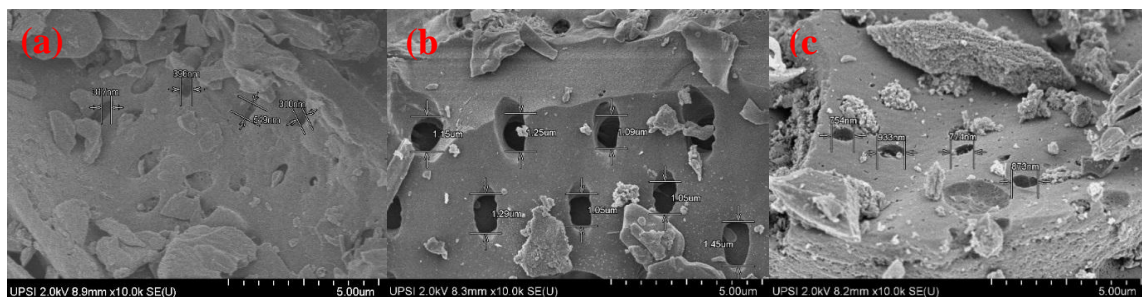


Figure 2: FESEM micrographs (a) agarwood before activation (b) agar AC and (c) commercial AC.

The produced agar AC samples were associated with a powder X-Ray diffractogram between the  $2\theta$  values of  $5\text{-}80^\circ$  (Figure 3a). In the case of each sample, the diffractogram displayed the occurrence of wide scattered peaks at about  $2\theta = 20\text{-}28^\circ$  and  $2\theta = 42, 62$  and  $77^\circ$ , which is classified as graphitic carbon (Abdulkareem-Alsultan et al., 2019; Abdulkreem-Alsultan et al., 2016). Furthermore, unlike the marked peaks associated with substances of high crystallinity, the wide and scattered peaks indicated that the examined samples were poorly crystalline and amorphous. The reason is the pyrolysis temperature is lower than that associated with graphite, which is more than  $2700^\circ\text{C}$  (Abdulkareem- Alsultan, 2016). (Abdulkareem-alsultan et al., 2018).

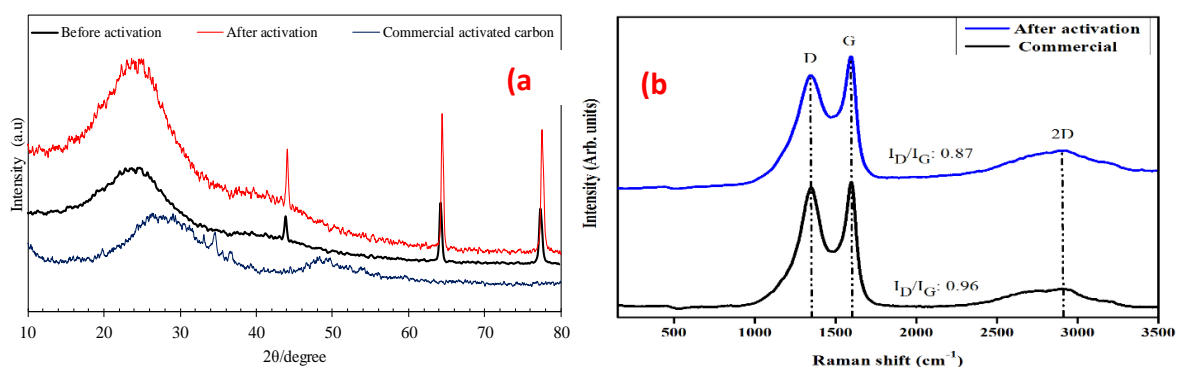


Figure 3: a) The X-ray diffraction profile of activated carbons and b) Raman Spectroscopy Agar AC commercial AC

The occurrence of abnormalities can be detected via Raman spectroscopy (Figure 3b), which was therefore applied to assess whether the produced agar AC samples contained a graphene layer or graphitic carbon. With regard to the identification of the morphological configuration of carbon materials, Raman spectroscopy possesses high sensitivity, and every band within the Raman spectrogram is associated with a specific vibrational frequency of a bond within the molecule. The D band was observed at 1348.96 and 1348.55  $\text{cm}^{-1}$  of agar AC after activation and commercial activated carbon, respectively. The boarded of D band observed in commercial activated carbon compared to agar AC after activation, which was 238.77 and 205.73  $\text{cm}^{-1}$ , respectively. This was suggested higher defection and disorder of commercial activated carbon compare to agar AC after activation. In addition, the G band of commercial activated carbon was observed at 1597.57  $\text{cm}^{-1}$ . The G band shows the width of commercial activated carbon was  $\sim 128.64 \text{ cm}^{-1}$ . Furthermore, the  $I_D/I_G$  ratio of commercial activated carbon was  $\sim 0.96$ . The higher  $I_D/I_G$  observed in the commercial activated carbon compare to agar AC after activation. This was believed due to higher defection and low crystallinity as confirmed by FESEM images (ref Figure 3a). Thus, the agar AC after activation shows higher crystallinity structure compare to commercial activated carbon. This suggested the agar AC after activation present higher performance than commercial activated carbon. Meanwhile, the commercial activated carbon shows the 2D band at 2919.64  $\text{cm}^{-1}$  with width 836.64  $\text{cm}^{-1}$ . The boarded 2D band observed in commercial activated carbon compare to agarAC after activation. This was suggested due to the thick layer of commercial activated carbon than agar AC after activation. Thus, the agar AC after activation present higher crystallinity and good structure compare to commercial activated carbon. Moreover, The structures of agar AC after activation and commercial activated carbon were investigated by micro-Raman spectroscopy as shown in Figure 3b The D band was observed at 1348.96 and 1348.55  $\text{cm}^{-1}$  of agar AC after activation and commercial activated carbon, respectively. This suggested the agar AC after activation present higher performance than commercial activated carbon.

### Batch Adsorption Experiments

The batch adsorption experiment by using agarAC was carried out and optimized using OVAT method to investigate the effect of carbon dosage, contact time, pH and temperature. The effect of mass dosage of agarAC was investigated in the range of 0.5-5 wt. % with other process parameters kept constant. The obtained results are as shown in Figure 4a, it can be seen that there is a significant sorption rate increase that correlates with the dosage increase from 0.5 to 1 wt.% It is likely that this is due to an incremental increase in surface area, which corresponds with an increase in the availability of active binding sites. Interestingly, in this study, further loading of agar AC beyond 1 wt.% resulted in a notable decrease in the adsorption of BPA. This is probably due to overlapping of adsorption sites resulting from overcrowding of agarAC particles. The amount of BPA adsorbed increases by increasing the adsorbent dosage but, the quantity adsorbed per unit mass decreases. There is a decrease in adsorption density with an increase in adsorbent mass because of unsaturated adsorption sites during the adsorption process, whereas the number of sites available for adsorption site increased by an increment in agarAC dosage. This phenomenon was observed by Pathania, Sharma, and Singh (2017).

The influence of contact time on BPA adsorption onto agarAC was studied (figure 4b). This to investigate contact time effect on adsorption process and establish equilibrium time required for maximum BPA uptake and adsorption process kinetics. The extent of BPA adsorbed at varied contact time were obtained by keeping agarACdosage, initial BPA concentration and temperature constant at 1 wt. %,pH=7 ,Temperature 50 °C.and250 mg/L respectively, and the results obtained were presented in Figure 4. The BPA removal was found to significantly increase by increasing the time from 30 to 350 min. Thus, the optimum or equilibrium time was taken to be 350 min. The higher the reaction time, the stronger the adsorbate-adsorbent bonds and the higher the adsorption efficiency. The significant steady desorption rate was due to the fact that large surface areas of agar AC carbonwere available at the beginning for BPA sorption (Akazdam et al., 2017). Contaminant sorption in water also depends on pH, which can impact not only the sorbent surface charge but the dominant sorbate form as well (Wang et al., 2017, Pathania, Sharma & Singh, 2017). Figure 4c shows how BPA adsorption on AC is impacted by pH; it can be observed that the levels of BPA adsorption on AC were increased as the pH increased from 3 to 7, but they declined quickly in the pH range 7-11. Surface deprotonation is the likely reason for the reduction in AC surface charge with pH increase, given the hypotheses formulated by Pathania, Sharma and Singh (2017). Moreover, at a pH lower than 8, BPA manifests in its neutral or molecular form, while at pH 8 or higher, it starts to undergo deprotonation to a form with a negative charge (Wang et al., 2017; Fang et al., 2018). Therefore, at a pH greater than 7, the bisphenolate anion and the agar AC surface with negative charge can have a repulsive electrostatic interaction, which would diminish the adsorption capability of BPA, as shown in the present study (Figure 4c).

Figure 4d shows the outcomes of the investigation of how bisphenolA adsorption on agarAC was affected by temperature, under conditions of varying temperature (30 to 50°C) and fixed dosage and time. The increase in temperature from 30 to 50°C led to enhanced adsorption of BPA and the exothermic nature of the adsorption was suggested by the fact that the maximum adsorption capacity ( $Q_m$ ) was obtained at 50°C. Thus, temperature increase may improve adsorption capacity and therefore enhance the adsorptive forces among bisphenol A and agarAC surface active sites (Ifelebuegu et al., 2015, Park et al., 2010), Hence, 50°C was taken as the optimum temperature for adsorption of BPA to agar AC in all subsequent experiments (Figure 4d).

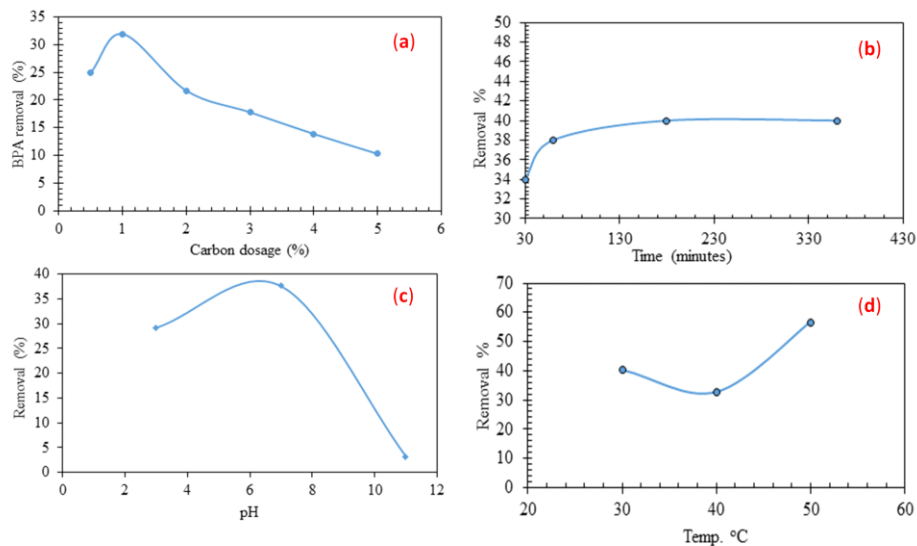


Figure 4: Optimization study for BPA on agar activated carbon: a) Effect of carbon content, b) Effect of contact time, c) Effect of initial solution pH on BPA adsorption and d) Effect of temperature on BPA adsorption

#### Adsorption Isotherm Study

Isotherms studies area helpful tool in the designing of an accurate model for the removal of contaminants from liquid media. It is resourceful to predict the adsorbent effectiveness towards a given pollutant in wastewater. Precise representation of equilibrium data for design purpose by various isotherms models is essential. Adsorption isotherm study was performed at varying initial BPA concentrations and other variables kept constant as; 1 wt. % activated carbon load, pH 7, 24 hours contact time and 50 °C. Langmuir and Freundlich are the most widely accepted two-parameter isotherm models. These two cited adsorption isotherm models were employed to obtain fit to BPA adsorption by  $H_2SO_4$  treated agar AC and the result presented in Figure 5.

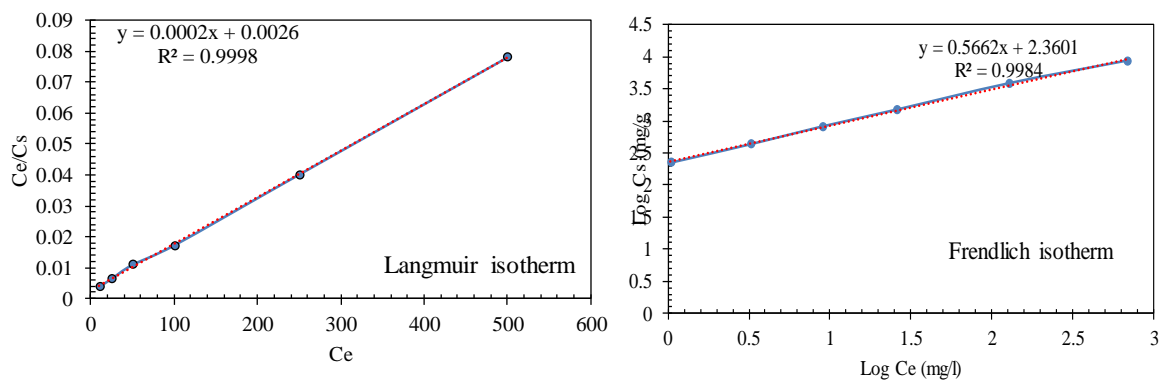


Figure 5: Langmuir and Freundlich Isotherm

The plot for Langmuir and Freundlich adsorption isotherms were presented in Figure 5, respectively to the BPA uptake data. The average value of separation factor  $R_L$  (an important parameter for Langmuir) was between 0.0002 and 0.043 suggested favourable adsorption of BPA-agarAC system. The value of  $n$  (1.78) indicated that physical process and multilayer adsorption are favourable according to Li and Gondal (Li & Gondal, 2014).

These results suggested that both Langmuir and Freundlich isotherms fit well for the equilibrium data. The maximum sorption capacity of prepared agar AC is 439 mg/g. Based on the correlation coefficient ( $R^2$ ) values (Table 1), both isotherm models suitably described the BPA adsorption process. It implied that BPA is chemically adsorbed to agar AC at fixed well-defined sites as well as heterogeneous surface interactions between BPA species (Bhatnagar & Anastopoulos, 2017; Kim et al., 2011; Sadaf et al., 2015). Besides, the adsorption capacity of agar AC towards BPA was the highest than other adsorbent reported according to Table 2

Table 1: Parameters of the Langmuir and Freundlich adsorption models for BPA molecules

Adsorbent	Langmuir model			Freundlich model		
	$q_{\max}$ (mg/g)	$K_L$ (L/mg)	$R^2$	$K_F$ ( $\text{mg}^{1-1/n}\text{L}^{1/n}\text{g}^{-1}$ )	$n$	$R^2$
Agar AC	439	1.041	0.9992	10.66	1.78	0.9992

#### Comparison between agarwood ACvs Commercial Activated Carbon

The surface charge for agar AC and commercial AC samples varied as depicted in Figure 6. At acidic medium (pH 3), the zeta potentials were -19.5 mV and -18.4 mV respectively for agar AC and commercial AC. Although, agar AC observed more negatively charged than commercial AC. The zeta potential values of the two samples become more negatively charged with an increase in pH values from acidic medium to an alkaline condition. In addition, the point zero charges for agar AC and commercial AC were not detected at all tested pH ranges (3 to 9), which indicates that the surfaces were negatively charged irrespective of pH. This is similar to Fahmi et al., report, no point zero charge detection for modified oil palm fruit bunch biochar (Fahmi et al., 2018).

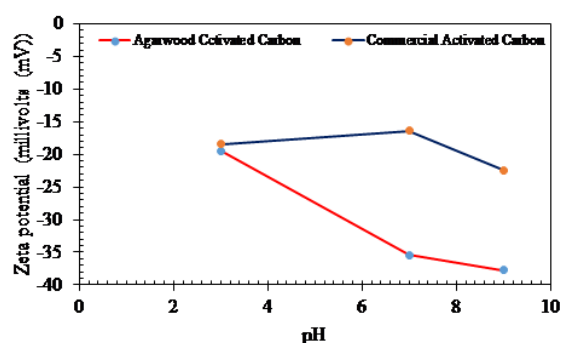


Figure 6: Zeta potential of (a) Agarwood AC and (b) commercial AC at different pH.

As presented in Figure 7, the agar AC has BPA adsorption capacities comparable to the commercial activated carbon. Adsorption efficiency increases as the BPA concentration increased and correlation factor  $R^2$  almost unity for prepared agar. This suggests that the agar AC carbon is a good alternative to expensive commercial activated carbons.

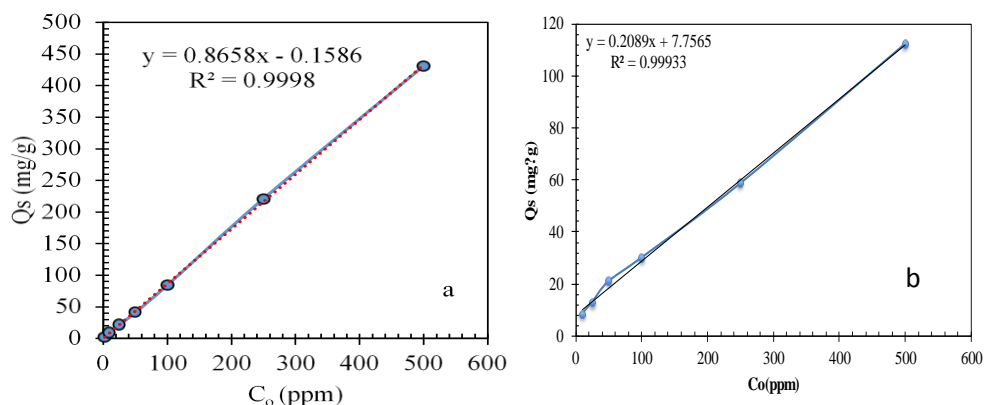


Figure 7: Adsorption capacity of (a) agar AC and (b) commercial AC towards BPA  
**BPA Adsorption Kinetics**

The data on the dependence of adsorption capacity with time was used for kinetic analysis. Pathania, Sharma and Singh (2017) utilised this method on their study on FCBC adsorption of methylene blue. They reported that the adsorption of methylene blue onto FCBC were applied to pseudo-first and

second-order kinetic models. In their study, they found that the correlation coefficient of the second-order kinetic model was greater than that of the first-order kinetic model. As such, they claim that this confirms that chemisorption is the rate-limiting step as this uses valence forces via the exchange or sharing of electrons. Figure 8 a and b, respectively, show the tests of pseudo-first-order and pseudo-second-order kinetic models:

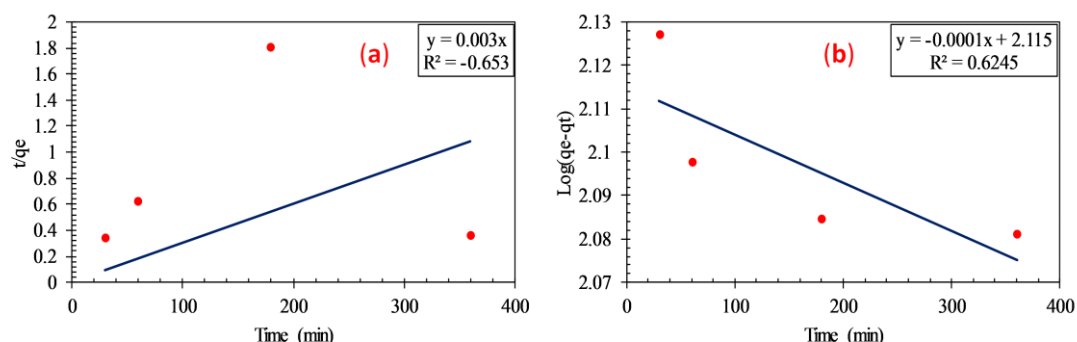


Figure 8: BPA adsorption kinetic; (a) Pseudo-first-order and (b) pseudo-second-order

Table 2 shows the outcomes of data fitting to the kinetic parameters of the pseudo-first-order and pseudo-second-order models, as well as the correlation coefficients  $R^2$ . When the empirical data were fitted with the Pseudo-first-order and pseudo-second-order kinetics, acceptable correlation coefficient  $R^2$  exceeding 0.653 and 0.6245 respectably, were achieved (Table 2). Moreover, there was good compatibility between the determined  $q_e$  values and the empirical data. It could thus be concluded that a pseudo-second-order kinetic model provided a more adequate characterisation of BPA adsorption by agar AC, while chemisorption was the dominant regulator of the process of adsorption.

Table 2: Coefficient of empirical kinetic models

time	$k(\text{min}^{-1})$	$\log(q_e - qt)$ (mg/g)	$t/q_e(\text{min.g/mg})$
30	0.500413	2.127105	0.344828
60	0.567953	2.097778	0.626632
180	0.598356	2.084576	1.809045
360	0.606622	2.080987	0.358209

## CONCLUSION

Agarwood branch was used for the production of the ideal surface area AC of 1092  $\text{m}^2/\text{g}$  and overall pore volume of 0.41  $\text{cm}^3/\text{g}$ . The highest capacity of bisphenol A (439  $\text{mg}/\text{g}$ ) was achieved by batch adsorption studies of BPA on agar AC under conditions of 50°C, pH 7 and three-hour time frame. Chemical adsorption was implied from the fact that the optimal characterisation of the empirical data was provided by the pseudo-second-order model ( $R^2$  correlation coefficient = 0.9994) and Elovich model ( $R^2$  correlation coefficient = 0.9999). The Langmuir and Dubinin-Radushkevich (D-R) adsorption models confirmed both the chemical and physical adsorption on AC. Furthermore, by comparison to commercial AC, agar AC showed promising adsorption capability. According to the results of the present study, it can be concluded that efficient adsorption of BPA assimilated from water and wastewater can be successfully achieved by using AC obtained from agarwood.

## REFERENCES

- [1] Abdulkareem-Alsultan, G., Asikin-Mijan, N., Lee, H.V., Rashid, U., Islam, A., & Taufiq-Yap, Y. H. (2019). A Review on Thermal Conversion of Plant Oil (Edible and Inedible) into Green Fuel Using Carbon-Based Nanocatalyst. *Catalysts*, 9(4), 1–25.
- [2] Abdulkareem-alsultan, G., Asikin-Mijan, N., Mansir, N., Lee, H. V., Zainal, Z., Islam, A., & Taufiq-Yap, Y.H. (2018). Pyro-lytic de-oxygenation of waste cooking oil for green diesel production over Ag2O3-La2O3/AC nano-catalyst. *Journal of Analytical and Applied Pyrolysis*, 137(2018), 171–184.
- [3] Abdulkreem-Alsultan, G., Islam, A., Janaun, J., Mastuli, M.S., & Taufiq-Yap, Y.H. (2016). Synthesis of structured carbon nanorods for efficient hydrogen storage. *Materials Letters*, 179, 57–60.
- [4] Acosta, R., Nabarlantz, D., Sánchez-Sánchez, A., Jagiello, J., Gadonneix, P., Celzard, A., & Fierro, V. (2018). Adsorption of Bisphenol A on KOH-activated tyre pyrolysis char. *Journal of environmental chemical engineering*, 6(1), 823–833.
- [5] Akazdam, S., Chafi, M., Yassine, W., Sebbahi, L., Gourich, B., & Barka, N. (2017). Decolourization of Cationic and Anionic Dyes from Aqueous Solution by Adsorption on NaOH Treated Eggshells :

- Batch and Fixed Bed Column Study using Response Surface Methodology. *Journal of Materials and Environmental Sciences*, 8(3), 784–800.
- [6] Arampatzidou, A.C., & Deliyanni, E.A. (2016). Comparison of activation media and pyrolysis temperature for activated carbons development by pyrolysis of potato peels for effective adsorption of endocrine disruptor bisphenol-A. *Journal of Colloid and Interface Science*, 466, 101–112.
- [7] Batra, S., Datta, D., Sai Beesabathuni, N., Kanjolia, N., & Saha, S. (2019). Adsorption of Bisphenol-A from aqueous solution using amberlite XAD-7 impregnated with aliquat 336: Batch, column, and design studies. *Process Safety and Environmental Protection*, 122, 232–246.
- [8] Berhane, T.M., Levy, J., Krekeler, M.P.S., & Danielson, N.D. (2016). Adsorption of bisphenol A and ciprofloxacin by palygorskite-montmorillonite: Effect of granule size, solution chemistry and temperature. *Applied Clay Science*, 518–527.
- [9] Bhatnagar, A., & Anastopoulos, I. (2017). Adsorptive removal of bisphenol A (BPA) from aqueous solution: a review. *Chemosphere*, 168, 885–902.
- [10] Chen, W., Pan, S., Cheng, H., Sweetman, A.J., Zhang, H., & Jones, K.C. (2018). Diffusive gradients in thin-films (DGT) for in situ sampling of selected endocrine disrupting chemicals (EDCs) in waters. *Water research*, 137, 211–219.
- [11] Choi, Y.K., & Kan, E. (2019). Effects of pyrolysis temperature on the physicochemical properties of alfalfa-derived biochar for the adsorption of bisphenol A and sulfamethoxazole in water. *Chemosphere*, 218, 741–748.
- [12] Dai, Y., Yao, J., Song, Y., Liu, X., Wang, S., & Yuan, Y. (2016). Enhanced performance of immobilized laccase in electrospun fibrous membranes by carbon nanotubes modification and its application for bisphenol A removal from water. *Journal of hazardous materials*, 317, 485–493.
- [13] Fahmi, A., Samsuri, A., Jol, H., & Advances, D.S.R. (2018). Undefined. (2018). Physical modification of biochar to expose the inner pores and their functional groups to enhance lead adsorption. *Pubs. Rsc. Org*, 38270–38280.
- [14] Genç, N., Kılıçoğlu, Ö., & Narci, A.O. (2017). Removal of Bisphenol A aqueous solution using surfactant-modified natural zeolite: Taguchi's experimental design, adsorption kinetic, equilibrium and thermodynamic study. *Environmental Technology (United Kingdom)*, 38(4), 424–432.
- [15] Kim, Y. H., Lee, B., Choo, K. H., & Choi, S. J. (2011). Selective adsorption of bisphenol A by organic-inorganic hybrid mesoporous silicas. *Microporous and Mesoporous Materials*, 138(1-3), 184–190.
- [16] Lassouane, F., Aït-Amar, H., Amrani, S., & Rodriguez-Couto, S. (2019). A promising laccase immobilization approach for Bisphenol A removal from aqueous solutions. *Bioresource technology*, 271, 360–367.
- [17] Li, Z., Gondal, M.A., & Yamani, Z.H. (2014). Preparation of magnetic separable CoFe<sub>2</sub>O<sub>4</sub>/PAC composite and the adsorption of bisphenol A from aqueous solution. *Journal of Saudi Chemical Society*, 18(3), 208–213.
- [18] Michałowicz, J. (2014). Bisphenol A—sources, toxicity and biotransformation. *Environmental toxicology and pharmacology*, 37(2), 738–758.
- [19] Pachamuthu, M. P., Karthikeyan, S., Maheswari, R., Lee, A.F., & Ramanathan, A. (2017). Fenton-like degradation of Bisphenol A catalyzed by mesoporous Cu/TUD-1. *Applied Surface Science*, 393, 67–73.
- [20] Pathania, D., Sharma, S., & Singh, P. (2017). Removal of methylene blue by adsorption onto activated carbon developed from Ficus carica bast. *Arabian Journal of Chemistry*, 10, S1445–S1451.
- [21] Sadaf, S., Bhatti, H. N., Nausheen, S., & Amin, M. (2015). Application of a novel lignocellulosic biomaterial for the removal of Direct Yellow 50 dye from aqueous solution: batch and column study. *Journal of the Taiwan Institute of Chemical Engineers*, 47, 160–170.
- [22] Shafei, A., Matbouly, M., Mostafa, E., Al Sannat, S., Abdelrahman, M., Lewis, B., ... & Mostafa, R. M. (2018). Stop eating plastic, molecular signaling of bisphenol A in breast cancer. *Environmental Science and Pollution Research*, 25(24), 23624–23630.
- [23] Zhang, H., Ma, S., Li, Y., Ou, J., Wei, Y., & Ye, M. (2019). Thiol-ene polymerization for hierarchically porous hybrid materials by adding degradable polycaprolactone for adsorption of bisphenol

- A. *Journal of hazardous materials*, 367, 465-472.
- [24] Zheng, S., Sun, Z., Park, Y., Ayoko, G. A., & Frost, R. L. (2013). Removal of bisphenol A from wastewater by Ca-montmorillonite modified with selected surfactants. *Chemical engineering journal*, 234, 416-422.
- [25] Zhu, H., & Li, W. (2013). Bisphenol A removal from synthetic municipal wastewater by a bioreactor coupled with either a forward osmotic membrane or a microfiltration membrane unit. *Frontiers of Environmental Science & Engineering*, 7(2), 294-300.